AFOSR TR-75-1600

Approved for public release; distribution unlimited.

ESL-P-622

THE STOCHASTIC CONTROL OF THE F-8C AIRCRAFT USING THE MULTIPLE MODEL ADAPTIVE CONTROL (MMAC) METHOD*

M. Athans, K-P. Dunn, C. S. Greene, W. H. Lee, N. R. Sandell, Jr., I. Segall and A. S. Willsky
Electronic Systems Laboratory
Massachusetts Institute of Technology
Cambridge, Massachusetts 02139

12p.

AF-AFOSR-2273-72,
NGL-22-009-124

Abstract

The purpose of this paper is to summarize results obtained for the adaptive control of the F-8C aircraft using the so-called MMAC method. The discussion includes the selection of the performance criteria for both the lateral and the longitudinal dynamics, the design of the Kalman filters for different flight conditions, the "identification" aspects of the design using hypothesis testing ideas, and the performance of the closed loop adaptive system.

1. Introduction

The purpose of this paper is to present preliminary results on a study which involves the application of advanced adaptive control techniques to the design of a stability augmentation system in both the longitudinal and lateral dynamics of the F-8C aircraft. NASA has been using the F-8C aircraft as a test vehicle for evaluating different digital-fly-by-wire (DFBW) control techniques, using the IBM AP-101 as the airborne computer. We remark that the eventual implementation of the control algorithms on the specific airborne computer has had a major impact upon the philosophy adopted for the design of the control system in view of the obvious storage and real-time computational constraints. In addition, the design was crucially dependent upon the sensors that could be utilized in the sense that sensors that utilized external aerodynamic measurements, e.g., airspeed, altitude, angle of attack and sideslip vanes should not be employed in the candidate design. Thus, the design guidelines required that the sensors associated with the adaptive control system should be limited to accelerometers, rate gyros, and perhaps attitude sensors (although the latter were deemed undesirable in view of their errors when the aircraft underwent severe pilot induced maneuvers).

From the viewpoint of modelling, it is obvious that the dynamic state equations of an aircraft involve nonlinear differential equations (see Etkin [1]). However, the information given by NASA Langley Research Center (LRC) to the MIT/ESL team consisted in the specification of the uncoupled, linear time-invariant open-loop longitudinal and lateral dynamics of the F-8C aircraft associated with equilibrium flight. Table I gives a list of the flight conditions that were available for the design. Thus, the general structure of the equations were of the form $\dot{x}(t)=Ax(t)+Bu(t)$. The numerical values of the elements of the A and B matrices can be found in a report by Gera [2], based upon wind tunnel tests, and a report by Wooley and Evans [3], based upon linearization of the nonlinear dynamics employed by NASA/LRC for their nonlinear simulation of the F-8C aircraft. We remark at this point that the numerical values for the A and B matrices given in [2] and [3] are not identical reflecting the fact that different sources were used to obtain them. The design reported in this paper is based upon Gera's report [2].

The fact that the 16 flight conditions span an extremely wide envelope for operating the aircraft, with drastic changes in the open-loop dynamics, makes the fixed-gain design of the control system unrealistic. Furthermore, handling qualities requirements, such as the C* criterion, indicate that pilots desire different closed-loop dynamics at different flight conditions. Thus, some sort of "adaptive" gain-scheduling control system was required. However, straight-forward gain scheduling based upon quantities such as velocity, altitude, and dynamic pressure was not permitted in view of the sensor restrictions mentioned above. Hence, the adaptive control system had to be designed in a novel way.

An additional restriction on the design was that the sensor noise and wind disturbances had to be incorporated. This led to the need for employing Kalman filters, with constant coefficients because of the computer memory limitations.

The above problem overview sets the ground for the specific adaptive control technique which we selected to investigate in great detail. We call the adaptive control technique the Multiple-Model-Adaptive-Control (MMAC) method, and we shall

*The theory and initial algorithm development associated with this study were developed with support from NASA/Ames Research Center under grant NGL-22-009-124 and from AFOSR under grant 72-2273. The specific application to the F-8C was supported by NASA Langley Research Center under grant NSG-1018.

Proceedings 1975 IEEE Conference on Decision and Control, Houston, Texas, December 1975

discuss it in more detail in Section 5 of this paper. It is only one of several techniques based upon developments in modern control theory (see the survey article by Athans and Varaiya [4]) and it has its origins in combining hypothesis-testing and stochastic control ideas (see references [4] to [8]). It was selected for this study because of its potential promise in academic examples [5]-[8], and because its memory and real-time computational requirements could be readily assessed in view of its non-iterative nature.

As explained in more detail in Section 5, the MMAC method requires that a full blown steady state Linear-Quadratic-Gaussian (LQG) controller be implemented for each flight condition. This necessitated the development of suitable quadratic performance criteria for both the longitudinal and the lateral dynamics; these are described for the continuous time case [9] in Sections 2 and 3, respectively. For implementation, one needs a discrete time LQG controller [10]. This is described in Section 4, together with the discussion of sensor errors. The MMAC algorithm is described in Section 5. The simulation results using the nonlinear F-8C dynamics are described in Section 6. Section 7 presents the major conclusion of our studies so far.

We remark that in this paper we shall only focus our attention to the regulation aspects of the problem, i.e., return to equilibrium flight from some initial conditions and in the presence of stochastic wind disturbances. In our study we are considering the proper way of incorporating human pilot inputs for both the longitudinal and lateral case. However, we shall not present in this paper any of the approaches and preliminary results for the pilot input case.

2. Longitudinal Dynamics

2.1 Introduction

In this section we present an overview of the LQG philosophy adopted for designing the regulator for the longitudinal dynamics. Attention is given in the development of the quadratic performance index and the subsequent model simplification using a short period approximation. The main concept that we wish to stress is that the quadratic performance criteria employed changed in a natural way with each flight condition. The surprising result was that the short period poles of the resultant longitudinal closed-loop system were characterized for all flight conditions by two constant damping ratios, one associated with all subsonic flight conditions and one associated with all supersonic flight conditions.

2.2 The Longitudinal State Description

Because of a rate constraint saturation on the elevator rate, the control variable selected was the time rate of change of the commanded elevator rate ($\dot{\delta}_{ec}(t)$). This was integrated to generate the actual commanded elevator position ($\delta_{ec}(t)$) which was introduced to a first order servo with a time constant of 1/12 seconds to generate the actual deviation of the elevator $\delta_e(t)$ from its trimmed value. The elevator was then related to the four "natural" longitudinal state variables namely pitch rate, q(t)(rad/sec), velocity error v(t)(ft/sec), perturbed angle of attack from its trimmed value, $\alpha(t)$(rad), and pitch attitude deviation from its trimmed value $\theta(t)$(rad), [2]. In addition, a wind disturbance state w(t) was included (see Appendix A). Thus the state vector $\underline{x}(t)$ for the longitudinal dynamics was characterized by seven components

$$(2.1)\quad \underline{x}'(t)\triangleq[q(t),\ v(t),\ \alpha(t),\ \theta(t),\ \delta_e(t),\ \delta_{ec}(t),\ w(t)]$$

and the control variable $\underline{u}(t)$ was the commanded elevator rate

$$(2.2)\quad \underline{u}(t)\triangleq\dot{\delta}_{ec}(t)$$

This led to a linear-time invariant characterization for each flight condition of the form

$$(2.3)\quad \dot{\underline{x}}(t)=\underline{A}_i\underline{x}(t)+\underline{B}\underline{u}(t)+\underline{L}_i\underline{\xi}(t)$$

where $\underline{\xi}(t)$ was zero mean white noise, generating the wind disturbance and accounting for random actuator errors. The elements of $\underline{A}_i$ and $\underline{L}_i$ changed with each flight condition while

$$(2.4)\quad \underline{B}=[0\ 0\ 0\ 0\ 0\ 1\ 0]'$$

2.3 The Longitudinal Cost Functional

In order to apply the standard steady state LQG procedure [9] a quadratic performance index has to be selected. The general structure of the index was

$$(2.5)\quad J=\int_0^\infty[\underline{x}'(t)\underline{Q}_i\underline{x}(t)+\underline{u}'(t)\underline{R}_i\underline{u}(t)]dt$$

Note that the weighting matrices $\underline{Q}_i$, $\underline{R}_i$ had to be different from flight condition to flight condition reflecting in a natural way that the pilot wants different handling qualities as the speed (and dynamic pressure) changes.

In the initial design it was decided that one should relate the maximum deviations of

- o pitch attitude, θmax
- o pitch rate, qmax
- o normal acceleration, a_{nz}max
- o maximum commanded elevator rate, $\dot{\delta}_{ec}$max

resulting in the following structure of the performance criterion

$$(2.6)\quad J_{1,LON}=\int_0^\infty\left[\frac{a_{nz}^2(t)}{a_{nzmax}^2}+\frac{q^2(t)}{q^2max}+\frac{\theta^2(t)}{\theta^2max}+\frac{\dot{\delta}_{ec}^2(t)}{\dot{\delta}_{ecmax}^2}\right]dt$$

The normal acceleration $a_{nz}(t)$, in g's, was not used as a state variable. However, it is linearly related to some of the longitudinal state variables according to the formula

$$(2.7)\quad a_{nz}(t)=\frac{Vo}{g}\left[k_1\ v(t)+K_2\alpha(t)+K_3\delta_e(t)\right]\text{ in g's}$$

V_θ being the equilibrium speed. The constants k_1, k_2, k_3 can be calculated from the open loop $\underline{A}_1$ matrices, and hence change with flight condition. Effectively the structure of the criterion (2.6) implies that if at t=0 the maximum values of acceleration, pitch rate, or pitch attitude occurred, then one would be willing to saturate the elevator rate to remove them. For the preliminary design the following numerical values were selected (with the help of T. Elliott and J. Gera)

$$(2.8)\quad a_{nzmax}=6g\text{'s},\ q_{max}=10g/V_\theta,\ \theta_{max}=6g/V_\theta a_{33},\ \dot{\delta}_{ecmax}=0.435\ \text{rad/sec}$$

where a_{33} is the (3,3) element of the open loop longitudinal $\underline{A}_1$ matrix.

Roughly speaking, this criterion means that one is willing to saturate the elevator rate (0.435 rad/sec for the F-8C) if a normal acceleration of 6g was felt, or a pitch rate equivalent to 10g's, or a pitch error which if translated to angle of attack would also generate a 6g normal acceleration.

The above numerical values were translated into the appropriate $\underline{Q}_1$ matrix (non diagonal positive semidefinite) which changed from flight condition to flight condition, while $\underline{R}_1=\underline{P}=1/(0.435)^2$ for all flight conditions. Hence, the resulting LQG problem could be solved using available computer subroutines [11].

2.4 Reduced Longitudinal Design

The design was modified for two reasons. First the gain from the velocity state variable v(t) was extremely small. Second, it was desirable to avoid using the pitch sensor. The pitch $\theta(t)$ is weakly observable from the system dynamics so that even if a Kalman filter was used in the absence of pitch measurements, large estimation errors would be obtained which would adversly affect the performance of the control system since there is significant feedback from the estimated pitch attitude. At any rate, since a pilot would fly the aircraft he would be able to control pitch himself.

This led us to eliminating the velocity error v(t) and pitch $\theta(t)$ from the state equations and obtaining the "short period" approximation (5 state variables). Since pitch did not appear the criteria (2.6) was modified to

$$(2.9)\quad J_{2,LON}=\int_0^\infty \left[\frac{a_{nz}^2(t)}{a_{nzmax}^2}+\frac{q^2(t)}{q^2_{max}}+\frac{\dot{\delta}_{ec}^2(t)}{\dot{\delta}^2_{ecmax}}\right]dt$$

and the resultant LQG problem was resolved.

2.4 Summary of Results

From the viewpoint of transient responses to the variables of interest (normal acceleration, pitch rate, angle of attack) the transient responses to initial conditions were almost identical for both designs. Thus, the short period motion of the aircraft was dominated by the relative tradeoff between the maximum normal acceleration, a_{nzmax}, and maximum pitch rate, q_{max}. This is consistent with the C^0 criterion [12].

When the short-period closed-loop poles were evaluated for both designs using the numerical values given by (2.8), we found the unexpected result that the damping ratio was constant (0.486) for all 11 subsonic flight conditions, and also constant (0.361) for all the supersonic flight conditions. The closed-loop naturally frequency increased with dynamic pressure.

Since no pole-placement techniques were employed (i.e., the mathematics were not told to place the closed-loop poles on a constant damping ratio line), we constructed a tradeoff by changing (decreasing) the maximum pitch rate q_{max}. This would increase the pitch rate penalty in the cost functional, and one would expect a higher damping ratio. The following values of q_{max} were employed

$$(2.10)\quad q_{max}=10g/V_\theta,\ 8g/V_\theta,\ 6g/V_\theta,\ 4g/V_\theta$$

Once more the constant damping ratio phenomenon was observed, i.e., for each value of q_{max} the short period closed loop poles for all subsonic flight conditions fell on a constant damping ratio line, and similarly for all supersonic flight conditions. This was further verified by considering an additional 13 different flight conditions.

The numerical results are presented in Table II. The reason for this regularity of the solution of the LQ problem is under investigation.

3. Lateral Dynamics

3.1 Introduction

In this section we present the parallel philosophy for the development of the control system for the lateral dynamics. In this case the development of a performance criterion was not as straight-forward as in the case of the longitudinal dynamics. For an extensive discussion see the S.M. thesis by Greene [13].

3.2 The Lateral Dynamics State Model

The control variables selected for lateral control were

$$(3.1)\quad u_1(t)=\dot{\delta}_{ac}(t)=\text{commanded aileron rate (rad/sec)}$$

$$(3.2)\quad u_2(t)=\dot{\delta}_{rc}(t)=\text{commanded rudder rate (rad/sec)}$$

so that the control vector is defined to be

$$(3.3)\quad \underline{u}^1(t)=[u_1(t)\quad u_2(t)]$$

The servomechanics were taken into account. The commanded aileron and rudder rates were integrated to generate the commanded aileron ($\delta_{ac}(t)$) and rudder ($\delta_{rc}(t)$) positions, respectively. For the

F-8C aircraft the commanded aileron rate $\delta_{ac}(t)$ drives a first order lag servo, with a time construct of 1/30 seconds, to generate the actual aileron position $\delta_a(t)$ (rads).

The commanded rudder rate $\delta_{rc}(t)$ (rads) drives a first order lag servo, with a time constant of 1/25 seconds, to generate the actual rudder position $\delta_r(t)$ (rads). The actual aileron and rudder position, $\delta_a(t)$ and $\delta_r(t)$, then excite the four "natural" lateral dynamics state variables, namely roll-rate p(t) (rad/sec), yaw-rate r(t) (rad/sec), sideslip angle $\beta(t)$ (rad), and bank angle $\phi(t)$ (rad). In addition, a wind disturbance state variable w(t), see Appendix A, drives the equations in the same way as the sideslip variable.

Thus, the state equations for the lateral dynamics are characterized by a 9-dimensional state vector $\underline{x}(t)$ with components

$$(3.4)\quad \underline{x}'(t) \triangleq [p(t)\ r(t)\ \beta(t)\ \phi(t)\ \delta_a(t)\ \delta_r(t)\ \delta_{ac}(t)\ \delta_{rc}(t)\ w(t)]$$

and the overall lateral dynamics take the form

$$(3.5)\quad \dot{\underline{x}}(t) = \underline{A}_i \underline{x}(t) + \underline{B}\,\underline{u}(t) + \underline{L}_i \underline{\xi}(t)$$

where the zero mean white noise vector $\underline{\xi}(t)$ generates the wind disturbance and compensates for modelling errors. Once more the matrices $\underline{A}_i$, $\underline{L}_i$ change with flight conditions [2], [13] while

$$(3.6)\quad \underline{B}' = \begin{bmatrix} 0 & 0 & 0 & 0 & 0 & 0 & 1 & 0 & 0 \\ 0 & 0 & 0 & 0 & 0 & 0 & 0 & 1 & 0 \end{bmatrix}$$

3.3 The Lateral Cost Functional

The lateral performance index used (after several iterations) weighted the following variables:

- o lateral acceleration, $a_y(t)$ (in g's)
- o roll rate, p(t) (in rad/sec)
- o sideslip angle, $\beta(t)$ (in rad)
- o bank angle, $\phi(t)$ (in rad)

VS

- o commanded aileron rate, $\dot{\delta}_{ac}(t)$
- o commanded rudder rate, $\dot{\delta}_{rc}(t)$

The lateral acceleration, $a_y(t)$, is not a state variable. However, for small perturbations from equilibrium flight, it can be expressed as a linear combination of the lateral state variables and the trim angle of attack, α_0, by the following relation

$$(3.7)\quad a_y(t) = \frac{V_0}{g}\,[(k_1-\alpha_0)p(t) + (k_2+1)r(t) + k_3\beta(t) + k_4\phi(t) + k_5\delta_r(t)] - \phi(t)$$

where the constants $k_1, \ldots, k_5$ can be found from the lateral open loop $\underline{A}_i$ matrix, and change with the flight condition.

The following structure of the quadratic performance criterion was established:

$$(3.8)\quad J_{LAT} = \int_0^\infty \frac{a_y^2(t)}{a_{ymax}^2} + \frac{p^2(t)}{p_{max}^2} + \frac{\beta^2(t)}{\beta_{max}^2} + \frac{\phi^2(t)}{\phi_{max}^2} + \frac{\dot{\delta}_{ac}^2(t)}{\dot{\delta}_{acmax}^2} + \frac{\dot{\delta}_{rc}^2(t)}{\dot{\delta}_{rcmax}^2}\ dt$$

The following maximum values were used

Maximum lateral acceleration, $a_{ymax} = 0.25g$'s

Maximum roll rate, $p_{max} = \frac{4V_0}{\sqrt{10g}}(a_{31} - \alpha_0)$

Maximum sideslip angle, $\beta_{max} = \frac{4V_0}{\sqrt{10g}}a_{33}$

Maximum bank angle, $\phi_{max} = 0.8$ rad ($=45°$)

Maximum commanded aileron rate = 1.63 rad/sec

Maximum commanded rudder rate = 1.22 rad/sec

See [13] for an extensive discussion of how this performance criterion was derived; a_{31} and a_{33} are obtained from the open loop $\underline{A}_i$ matrices

There is no natural way of arriving at a simplified model for the lateral dynamics, as was the case with the longitudinal dynamics. Hence the bank angle cannot be eliminated. Although a bank angle sensor was deemed undesirable, the weak observability of the bank angle caused large state estimation errors, using Kalman filters, in the bank angle and the sideslip angle if a bank angle sensor was not included. For these reasons, it was decided to employ a bank angle sensor and to penalize bank angle deviation, because bank angles larger than 20° can introduce significant nonlinearities through trigonometric functions [1].

Once more, the LQ can be solved. Notice that the use of the performance criterion (3.8) results in a state weighting matrix $\underline{Q}_i$ (non-diagonal) which changes with flight condition.

3.4 Summary of Results

The above performance criterion gave reasonable responses for a variety of initial conditions. Its main characteristic is to reduce any lateral accelerations (by forcing the aircraft to go in coordinated turns) and to null out bank angle errors in a slower manner.

Once more we observed a constant damping ratio (.515) for all supersonic conditions and a relatively constant damping ratio (.625) for all subsonic flight conditions. No additional tradeoff studies were conducted by changing the weights in the cost functional.

4. Sensors, Kalman Filters and Discrete LQG Compensators

4.1 Introduction

The digital implementation of the control system requires the discrete-time solution of the LQG problem [10]. As we shall see in the next section, the MMAC approach requires the construction of a bank of LQG controllers, each of which contains a discrete Kalman filter (whose residuals are used in probability calculations and whose state estimates are used to generate the adaptive control signals). Hence, in this section we present an overview of the issues involved in the design of the LQG controllers based upon the noisy sensor measurements.

4.2 The Sampling Interval

A sampling rate of 8 measurements/second was established. Such a slow sampling rate was selected so as to be able to carry out in real time the multitude of real time operations required by the MMAC method.

4.3 Sensors and Noise Characteristics

As explained in the introduction, the guidelines for design excluded the use of air data sensors. Thus, measurements of altitude, speed, angle of attack, and sideslip angle were not available. After some preliminary investigations it was decided that sensors that depend on trim variables (elevator angle and pitch attitude) should not be used so as to avoid estimating trim parameters. Table III lists the sensors and their accuracy characteristics that were used in this study. We stress that the sensors measure the true variables every 1/8 seconds in the presence of discrete-zero mean white noise with the standard deviations given in Table III.

Finally, we remark that in this study we assumed that all sensors were located at the C.G. of the aircraft.

4.4 The Design of Kalman Filters

For each flight condition the steady-state discrete-time Kalman filter, with constant gains was calculated, for both the longitudinal and lateral dynamic models. The level of the plant white noise associated with the wind disturbance generation was selected so that we assumed that the aircraft was flying in cumulus clouds. (See Appendix A.)

The decision to use steady state constant gain Kalman filters was made so as to minimize the computer memory requirements.

Finally, we remark that in view of the slow sampling rate, the continuous time filtering problem was carefully translated into the equivalent discrete problem [13] to [15].

The constant covariance matrices of the Kalman filter residuals, denoted by $\underline{S}_{iLON}$, $\underline{S}_{iLAT}$ for the longitudinal models and lateral models were computed for each flight condition denoted by i. As we shall see these are important in the generation of the MMAC variables.

4.5 The Design of the Discrete LQG Compensators

Through the use of the separation theorem one can design the discrete LQG compensators. This implied that the LQ problem defined in continuous time in Sections 2 and 3 had to be correctly transformed into the equivalent discrete-time problem in view of the slow measurement rate. Effectively, we have used the transformations given in references [11], [13] to [15].

4.6 Recapitulation

For each flight condition, indexed by i, a complete discrete-time, steady state, LQG compensator was designed for both the longitudinal and lateral dynamics. Each compensator generated every 1/8 second the optimal control, namely the optimal commanded elevator rate $\delta^i_{ec}(t)$ for the longitudinal dynamics, and the optimal commanded aileron rate $\delta^i_{ac}(t)$ and rudder rate $\delta^i_{rc}(t)$, based upon the noisy measurements of the appropriate sensors (See Table III) every 1/8 second.

Because of the appropriate transformations of the continuous time LQG problem to the discrete one, we noted no significant degradation in performance at this low sampling rate.

The need for adaptive control is obvious because if we assume that the aircraft is in flight condition i, but we use the LQG compensator obtained for flight condition j for feedback control, this mismatching may generate either an unstable system or, often, a system with degraded performance.

5. The MMAC Method

5.1 Introduction

In this section we present the basic idea behind the MMAC method, and discuss how it was used in the F-8C context. In particular, we demonstrate how the information generated by the lateral and longitudinal sensors is blended together. Finally we make some remarks associated with the MMAC method and its general applicability to the design of adaptive control systems.

5.2 The Basic Idea

Suppose one has N linear, discrete-time stochastic time-invariant dynamic systems, indexed by i=1, 2, ..., N, generating discrete-time measurements corrupted by white noise
Suppose that at t=0 "nature" selects one of these systems and places it inside a "black box." The true system generates a discrete set of measurements $\underline{z}(t)$. The objective is to apply a control signal $\underline{u}(t)$ to the true model.

The version of the MMAC method employed is as follows: one constructs a discrete-time steady state LQG controller for each model; thus, one has a bank of N LQG compensators. As shown in Figure 1, each LQG compensator is driven by the actual control applied to the system, $\underline{u}(t)$, and driven by the actual noisy measurement vector, $\underline{z}(t)$. There are two signals of interest that each LQG compensator generates at time t

(1) the control vector $\underline{u}_i(t)$, which would be the optimal control if indeed the system in the black box (viz. aircraft) was identical to the i-th model
(2) the residual or innovations vector $\underline{r}_i(t)$ generated by each Kalman filter (which is inside the i-th LQG compensator)

It turns out that (see references [4], [5], [6], [7], [8] for example) that from the residuals of the Kalman filters one can recursively generate N discrete time sequences denoted by $P_i(t)$, i=1, 2 ..., N, t=0, 1, 2, ..., which under suitable assumptions are the conditional probabilities at time t, given the past measurements $\underline{z}(\tau)$, $\tau \leq t$ and controls $\underline{u}(\sigma)$, $\sigma \leq t-1$, that the i-th model is the true one.

Assuming then that these probabilities are generated on-line (the formula will be given later) and given that each LQG compensator generates the control vector $\underline{u}_i(t)$, then as shown in Figure 1, the MMAC method computes the adaptive control vector $\underline{u}(t)$, which drives the true system (viz. aircraft) and each of the Kalman filters inside the LQG compensators, by probabilistically weighting the controls $\underline{u}_i(t)$ by the associated probabilities, i.e.,

$$(5.1) \quad \underline{u}(t) = \sum_{i=1}^{N} P_i(t)\underline{u}_i(t)$$

5.3 Calculation of the Probabilities $P_i(t)$

We assume that at t=0, i.e., before any measurements are obtained, one has a set of prior probabilities

$$(5.2) \quad P_1(0), \ldots, P_N(0), \; P_i(0) \geq 0, \; \sum_{i=1}^{N} P_i(0) = 1$$

that represent our "best guess" of which model is indeed the true one.

In our version of the MMAC method we have available the steady-state (constant) covariance matrix $\underline{S}_i$ of the residuals associated with the i-th Kalman filter. These N residual covariance matrices are precomputable. Let r denote the number of sensors; then we can precompute the N scalars

$$(5.3) \quad \beta_i \triangleq [(2\pi)^r \det \underline{S}_i]^{-1/2}$$

From the residual vector $\underline{r}_i(t)$ generated by each Kalman filter we generate on-line the N scalars

$$(5.4) \quad m_i(t) \triangleq \underline{r}_i'(t)\underline{S}_i^{-1}\underline{r}_i(t)$$

Then the probabilities at time t, $P_i(t)$, i=1, 2, ..., N are computed recursively from the probabilities at time t-1, $P_i(t-1)$, by the formula

$$(5.5) \quad P_i(t) = \frac{P_i(t-1)\beta_i \exp\{-m_i(t)/2\}}{\sum_{j=1}^{N} P_j(t-1)\beta_j \exp\{-m_j(t)/2\}}$$

with the initial probabilities, $P_i(0)$ given. It has been claimed that [5], [6], [8], under suitable assumptions that asymptotically the true model is identified with probability 1.

5.4 Important Remarks

1) It has been shown by Willner [8], that the MMAC method, i.e., generating the control via (5.1) is not optimal (it is optimal under suitable assumptions for the last stage of the dynamic programming algorithm).

2) The MMAC algorithm is appealing in an ad-hoc way because of its fixed structure and because its real-time and memory requirements are readily computable.

3) In the version used in this study, because we use steady-state Kalman filters, rather than time-varying Kalman filters, the $P_i(t)$ are not exactly the conditional probabilities.

4) We have been unable to find in the cited literature a rigorous proof of convergence of the claim that indeed the probability associated with the true model will asymptotically converge to unity.

5) From a heuristic point of view, the recursive probability formula (5.5) makes sense with respect to identification. If the system is subject to some sort of persistent exitation, then one would expect that the residuals of the Kalman filter associated with the correct model, say the i-th one will be "small," while the residuals of the mismatched Kalman filters ($j \neq i$, j=1, 2, ..., N) will be "large." Thus, if i indexes the correct model we would expect

$$(5.6) \quad m_i(t) << m_j(t) \quad \text{all } j \neq i$$

If such a condition presists over several measurements, the analysis of (5.5) shows that the "correct" probability $P_i(t)$ will increase while the "mismatched model" probabilities will decrease. To see this one can rewrite the formula (5.5) as follows

$$(5.7) \quad P_i(t) - P_i(t-1) = \left[\sum_{j=1}^{N} P_j(t-1)\beta_j \exp\{-m_j(t)/2\}\right]^{-1} \cdot$$

$$P_i(t-1)\left[(1-P_i(t-1))\beta_i \exp\{-m_j(t)/2\}\right]$$

$$- \sum_{j \neq i} P_j(t-1)\beta_j \exp\{-m_j(t)/2\}$$

Under our assumptions

(5.8) $\exp\{-m_i(t)/2\} \approx 1$

(5.9) $\exp\{-m_j(t)/2\} \approx 0$

Hence the correct probability will grow according to

$$(5.10)\quad P_i(t)-P_i(t-1) \approx \frac{P_i(t-1)[1-P_i(t-1)]\beta_i^*}{\sum_{j=1}^{N} P_j(t-1)\beta_j^* \exp\{-m_j(t)/2\}} > 0$$

which demonstrates that as $P_i(t) \to 1$, the rate of growth slows down.

On the other hand, for the incorrect models, indexed by $j \neq i$, the same assumptions yield

$$(5.11)\quad P_j(t)-P_j(t-1) \approx \frac{-P_j(t-1)P_i(t-1)\beta_i^*}{\sum_{k=1}^{N} P_k(t-1)\beta_k^* \exp\{-m_k(t)/2\}} < 0$$

so that the probabilities decrease.

The same conclusions hold if we rewrite (5.7) in the form

$$(5.12)\quad P_i(t)-P_i(t-1) = \left[\sum_{j=1}^{N} P_j(t-1)\beta_j^* \exp\{-m_j(t)/2\}\right]^{-1} \left[P_i(t-1)\sum_{j\neq i} P_j(t-1)\left(\beta_i^* \exp\{-m_i(t)/2\} - \beta_j^* \exp\{-m_j(t)/2\}\right)\right]$$

The above discussion points out that this "identification" scheme is crucially dependent upon the regularity of the residual behavior between the "matched" and "mismatched" Kalman filters.

(6) The "identification" scheme, in terms of the dynamic evolution of the residuals will not work very well if for whatever reason (including errors in the selection of the noise statistics) the residuals of the Kalman filters do not have the above regularity assumptions. Tobe specific, suppose that for a prolonged sequence of measurements the Kalman filter residuals turn out to be such that

$$(5.13)\quad m_1(t) \approx m_2(t) \approx \ldots \approx m_N(t)$$

Then

$$(5.14)\quad \exp\{-m_i(t)/2\} \approx \alpha \qquad \text{for all } i$$

Under these conditions and (5.12), we can see that

$$(5.15)\quad P_i(t)-P_i(t-1) \approx \frac{P_i(t-1)\sum_{j\neq i} P_j(t-1)(\beta_i^*-\beta_j^*)\alpha}{\sum_{j=1}^{N} P_j(t-1)\beta_j^*\alpha}$$

$$= \frac{P_i(t-1)\sum_{j\neq i} (\beta_i^*-\beta_j^*)P_j(t-1)}{\sum_{j=1}^{N} P_j(t-1)\beta_j^*}$$

Suppose that it turns out that one of the β_i^*'s, and to be specific β_k^*, is dominant, i.e.,

$$(5.16)\quad \beta_k^* > \beta_i^* \qquad \text{all } i \neq k$$

In this case, the RHS of eq. (5.15) will be negative for all $i \neq k$, which means that all the $P_i(t)$ will decrease while the probability P_k (associated with the dominant β_k^*) will increase. This behavior is very important, expecially when one lies to the mathematics, and it has not been discussed previously in the literature to the best of our knowledge.

5.5 Application to the F-8C

The MMAC method can be used in a straight forward manner using either the longitudinal or lateral dynamics of the F-8C aircraft since we have designed both longitudinal and lateral LQG compensators for the available flight conditions, as we remarked in Section 4.

On the other hand, we obtain independent information from the longitudinal and lateral systems for the same flight condition (i.e., model) indexed by i. Hence, it should be possible to blend this combined information into a set of single probabilities.

Under the assumption that the longitudinal and lateral dynamics are decoupled K-P Dunn derived the following relation.

Let $\underline{S}_{i\ LON}$ and $\underline{S}_{i\ LAT}$ denote the residual covariance matrices of the Kalman filters, for the i-th flight condition, associated with the longitudinal and lateral dynamics respectively. Define

$$(5.17)\quad \beta_i^*{}_{LON} = \left[(2\pi)^{r_{LON}} \det \underline{S}_{i\ LON}\right]^{-1/2}$$

$$(5.18)\quad \beta_i^*{}_{LAT} = \left[(2\pi)^{r_{LAT}} \det \underline{S}_{i\ LAT}\right]^{-1/2}$$

where r_{LON} and r_{LAT} are the number of longitudinal and lateral sensors. Let $\underline{r}_{i\ LON}(t)$ and $\underline{r}_{i\ LAT}(t)$ denote the Kalman filter residual vectors at time t, for flight condition i, associated with the longitudinal and lateral dynamics respectively. Define

$$(5.19)\quad m_{i\ LON} \triangleq \underline{r}_{i\ LON}'(t)\underline{S}_{i\ LON}^{-1}\underline{r}_{i\ LON}(t)$$

$$(5.20)\quad m_{i\ LAT} \triangleq \underline{r}_{i\ LAT}'(t)\underline{S}_{i\ LAT}^{-1}\underline{r}_{i\ LAT}(t)$$

Then the overall probability that the aircraft is in flight condition i at time t, is generated by the recursive formula

$$(5.21)\quad P_i(t)=\Big[P_i(t-1)\beta^*_{iLON}\beta^*_{iLAT}\cdot \exp\{-m_{iLON}(t)/2\}\exp\{-m_{iLAT}(t)/2\}\Big] \Big/ \Big[\sum_{j=1}^{N} P_j(t-1)\beta^*_{jLON}\beta^*_{jLAT}\cdot \exp\{-m_{jLON}(t)/2\}\exp\{-m_{jLAT}(t)/2\}\Big]$$

The β^* dominance effect discussed above now refers to the relative magnitude of

$$(5.22)\quad \beta_i^* \triangleq \beta_{i\,LON}^*\beta_{i\,LAT}^*$$

Obviously the method should be expected to work well when both longitudinal and lateral Kalman filters are correctly designed so that the residuals of the "matched" Kalman filters are smaller than those of the "mismatched" ones.

5.6 Discussion

It should be immediately obvious, that if the MMAC method is applied for the control of the F-8C aircraft (or any other physical system for that matter), one violates a multitude of theoretical assumptions. The effect of these upon the performance of the overall system is difficult to establish on an analytical basis, because the MMAC system, in spite of its simple structure, represents an extremely nonlinear system. Hence, one has to rely on extensive simulation results in order to be able to make a judgment of the performances of the overall algorithm.

Since the aircraft never coincides with the mathematical models (recall the discussion on the differences in the data given in references [2] and [3], the $P_i(t)$ are not truly posterior probabilities. Rather they should be interpreted as time sequences that have a reasonable physical interpretation. Hence, in our opinion, the evaluation of the MMAC method solely by the detailed dynamic evolution of the $P_i(t)$ is wrong. Rather it should be judged by the overall performance of the control system. In the case of the regulator, this is easy since one can always compare the response of the MMAC system with that which was designed explicitly for that flight condition and compare the results.

We remark that such a comparison is much more complex when one attacks the case of pilot inputs which result in several commanded maneuvers. These aspects are still under investigation.

There are several unresolved problems as yet which pertain to the total number of models to be used at each instant of time, how these models are to be selected, how they should be scheduled in the absence of any air data, and how one can arrive at a final design that meets the speed-memory limitations of the IBM AP-101 computer which is used in the NASA F-8C DFBW program.

We hope that some of the simulation results and discussion presented in the sequel can contribute some understanding upon the MMAC method as a design concept.

6 Simulation Results

6.1 Introduction

A variety of simulations have been done using both a linear model and nonlinear model of the F-8C aircraft. These simulations results are typical. They are selected such that they can demonstrate

1) the speed of identification of the MMAC algorithm;
2) the overall performance of the MMAC system; and
3) the β^* dominant behavior discussed in Section 5.

Some remarks about the MMAC method are given in the conclusions.

6.2 The Simulation Results

The simulations were conducted at a high altitude (40,000 ft), supersonic (Mach 1.4) flight condition (F/C #19 in Table I). No plant noise was introduced. All models available in the MMAC controller were given equal a priori probabilities being the true model.

Experiment #1:

This is a set of linear simulations with two degree sideslip angle (a β-gust) at time t=0. No sensor noise was introduced and the Kalman filters were set at the correct initial conditions.

Figure 2 shows the probability changes while the set of models available in the MMAC controller were F/C 8, 14, 18, 19 and 20. Note that the true filght condition was included in the controller. The correct model is initially chosen with high probability within a very short period of time (less than 1 sec.) and than switches to another model slowly after a few seconds. Lateral acceleration is removed within about one second, while roll rate and sideslip angle are reduced to zero almost as fast. With no noise perturbing the system, the states of the system have settled to near zero after about five seconds. Thus the residuals in all the mismatch stable filters approach zero. In this case the β^* dominant behavior discussed in Section 5 occurred. Figure 3 shows the probability changes when the true model (F/C #19) was not included (which was substituted by F/C #17). We observed the same β^* dominant behavior after about five seconds. The most important point to note is that responses of the MMAC system are almost identical. Figure 4 shows the responses of lateral acceleration with and without F/C #19 in the controller, respectively.

Similar results were obtained with other initial conditions. However, the speed with which the β^* starts to dominate varies greatly. For example, with a roll rate initial condition, it

happened much sooner. However, there is very little degradation in the overall system performance.

Experiment #2:

This is a set of nonlinear simulations with an initial six degree angle of attack (an α-gust). Sensor noise was introduced and the Kalman filters were set at zero initial conditions.

Figure 5 shows the change of probabilities when the set of models available in the MMAC controller were F/C 14, 17, 19, and 20 and when the true flight condition (F/C 19) was included. The probabilities are more active than those we have seen in Experiment #1. It is believed that the fast variation of these probabilities is due to a combination of the transient response of the system and the noise sequences on the sensors. However, the true flight condition is identified in about 1 second. The angle of attack returns to its trimmed value within about 2 seconds, while pitch rate and normal acceleration are reduced to zero almost as fast. In this case the β^* dominant behavior only occurs for a very short period of time. Because of the sensor noise, it is not certain if the drifting of probabilities are mainly due to the dominant β^*. Figure 6 shows the probability changes when F/C #19 (true) was substituted by F/C #18 in the MMAC controller. Again, the responses of the MMAC system are almost identical. Figure 7 shows the responses of the angle of attack with and without F/C #19 in the controller, respectively.

7. Conclusions

Based upon many simulations using both a linear model and a nonlinear model of the F-8C aircraft, there are several kinds of probabilities responses that one can guess before simulation, such as during the transient period the MMAC algorithm tends to pick F/C's which are mismatch stable while during the equilibrium condition the β^* dominant behavior tends to occur. However, a rigorous statement on the precise nature of the probability responses is still an open question. Other than the model identification problem, the overall performance of the MMAC method system is very good. Although poorly selected F/C's in the bank of Kalman filters may degrade the performance, the MMAC method seems to stabilize the system quite well. The β^* dominant problem is basically the same problem as in most parameter identification problems when there is lack of information.

Acknowledgments

This study was carried out under the overall supervision of Prof. M. Athans. The program manager was Dr. K-P Dunn, who had the major responsibility for coordinating the effort, developed the longitudinal control system and the overall MMAC system. Mr. C. S. Greene and Prof. A. S. Willsky were primarily responsible for the lateral system design. Prof. N. R. Sandell and Mr. W. H. Lee helped with the reduced order longitudinal design and Ms. I. Segall did much of the programming.

We are indebted to Mr. Jarrell R. Elliott of NASA/LRC who as grant monitor provided countless hours of technical discussions and direction and helped us formulate the performance criteria. In addition, we are indebted to the following staff of NASA/LRC for their help, criticism and support: R. Montgomery, J. Gera, C. Wooley, A. Schy and A. Evans.

References

1. B. Etkin, "Dynamics of Atmospheric Flight," Wiley, 1972.

2. J. Gera, "Linear Equations of Motion for F-8 DFBW Airplane at Selected Flight Conditions," NASA/Langley Research Center, Hampton, Va., F-8 DFBW Internal Document, Report No 010-74.

3. C. R. Wooley and A. B. Evans, "Algorithms and Aerodynamic Data for the Simulation of the F8-C DFBW Aircraft," NASA/Langley Research Center, Hampton, Va., (unpublished report dated Feb. 5, 1975).

4. M. Athans and P. P. Varaiya, "A Survey of Adaptive Stochastic Control Methods," Proc. Engineering Foundation Conference on Systems Engineering, New England College, Henniker, N. H., August 1975; also submitted to IEEE Trans. on Automatic Control.

5. D. T. Magill, "Optimal Adaptive Estimation of Sampled Processes," IEEE Trans. Automatic Control, Vol. AC-10, 1965, pp. 434-439.

6. J. D. Desphande, et al, "Adaptive Control of Linear Stochastic Systems," Automatica, Vol. 9, 1973, pp. 107-115.

7. M. Athans and D. Willner, "A Practical Scheme for Adaptive Aircraft Flight Control Systems," Proc. Symposium on Parameter Estimation Techniques and Applications in Aircraft Flight Testing, NASA TN D-7647, NASA Flight Research Center, Edwards, Calif., April 1973, pp. 315-336.

8. D. Willner, "Observation and Control of Partially Unknown Systems," MIT Electronic Systems Laboratory Report ESL-R-496, June 1973, Cambridge, Mass.

9. M. Athans, "The Role and Use of the Stochastic LQG Problem in Control System Design," IEEE Trans. Automatic Control, Vol. AC-16, 1971, pp. 529-552.

10. M. Athans, "The Discrete Time LQG Problem," Annals Economic and Social Measurement, Vol. 2, 1972, pp. 449-491.

11. N. R. Sandell, Jr. and M. Athans, "Modern Control Theory: Computer Manual for the LQG Problem," (can be ordered through the MIT Center for Advanced Engineering Study, Cambridge, Mass.

12. H. N. Tobie, E. M. Elliott, and L. G. Malcom, "A New Longitudinal Handling Qualities Criterion," presented at the 18th Annual National Aerospace Electronics Conference, 16-18 May, 1966.

13. C. S. Greene, "Application of the Multiple Model Adaptive Control Method to the Control of the Lateral Dynamics of an Aircraft," S. M. Thesis, Dept. of Electrical Engineering and Computer Sciences, MIT, Cambridge, Mass., May 1975.

14. A. H. Levis, "On the Optimal Sampled Data Control of Linear Processes," Sc.D. Thesis, Dept. of Mechanical Engineering, M.I.T., Cambridge, Mass., June 1968.

15. A. H. Levis, M. Athans, and R. Schlueter, "On the Behavior of Optimal Sampled Data Regulators," Int. J. Control, Vol. 13, 1971, pp. 343-361.

TABLE I

Flight Condition No.	Altitude (ft)	Mach No.	Dynamic Pressure (PSF)	Trim Angle of Attack (DEG.)	Trim Elevator (DEG.)
#5	Sea level	.3	133.2	7.991	-3.060
#6	Sea level	.53	416.0	2.980	-2.495
#7	Sea level	.7	726.0	1.921	-2.455
#8	Sea level	.85	1068.0	1.536	-2.37
#9	Sea level	1.0	1480.0	1.069	-1.673
#10	20,000	.4	109.0	9.270	-5.569
#11	20,000	.6	245.0	4.429	-3.663
#12	20,000	.8	434.0	2.626	-2.615
#13	20,000	.9	550.0	2.253	-2.650
#14	20,000	1.2	978.0	1.490	-2.131
#15	40,000	.7	135.0	7.035	-4.791
#16	40,000	.8	176.0	5.371	-3.891
#17	40,000	.9	223.0	4.257	-3.521
#18	40,000	1.2	397.0	2.872	-4.463
#19	40,000	1.4	537.0	2.736	-4.416
#20	40,000	1.6	703.0	2.063	-3.465

TABLE II

Damping ratio for closed-loop short period poles as a function of maximum pitch rate penalty, q_{max}, in (2.6) or (2.9)

q_{max}	Damping ratio for all subsonic conditions	Damping ratio for all supersonic conditions
$10q/V_o$	0.488	0.361
$8q/V_o$	0.530	0.402
$6q/V_o$	0.552	0.449
$4q/V_o$	0.587	0.498

TABLE III

Sensor Charasteristics

Variable	Symbol	Standard Deviation of additive white noise	
Pitch Rate	q	.489	Deg/sec
Normal acceleration	$a_{n,z}$	.06	g's
Roll Rate	p	1.056	Deg/sec
Yaw Rate	r	.489	Deg/sec
Bank angle	ϕ	1.0	Deg
Lateral acceleration	a_y	.04	g's

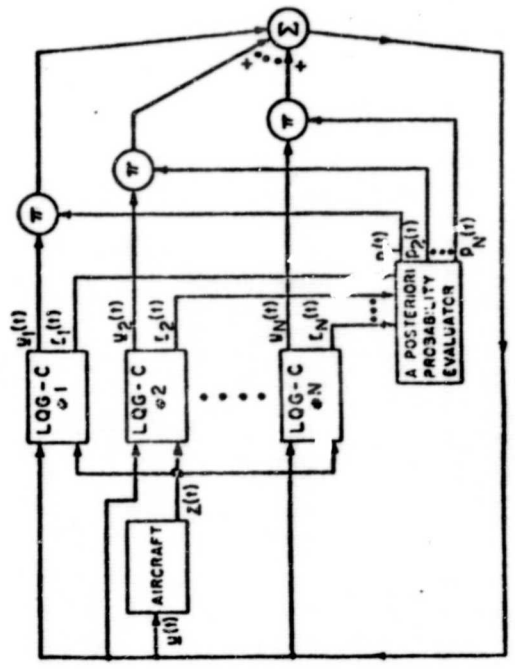

Figure 1 Structure of MMAC System

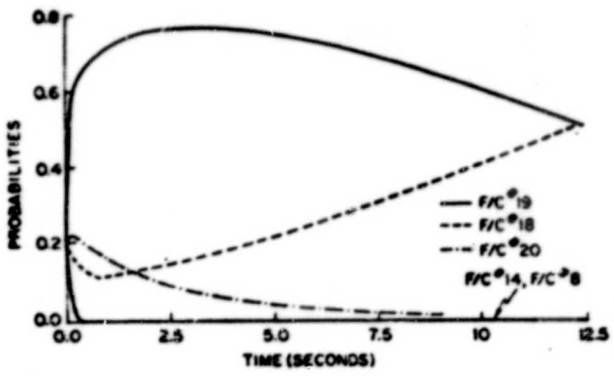

Figure 2 Probabilities Versus Time (true F/C #19 included) from Lateral Dynamics

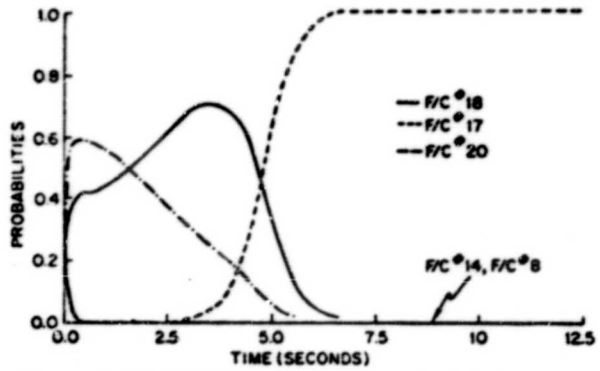

Figure 3 Probabilities Versus Time (true F/C #19 not included) from Lateral Dynamics

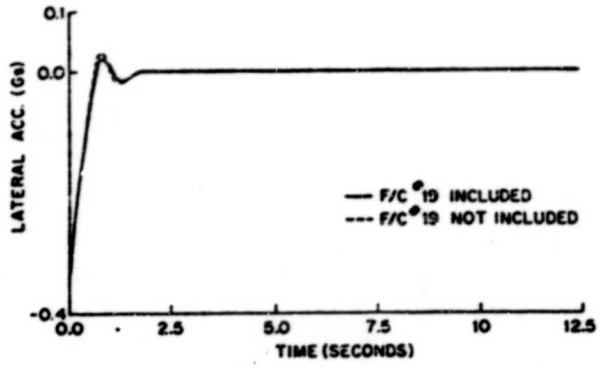

Figure 4 Lateral Acceleration Versus Time Using Lateral Information Only

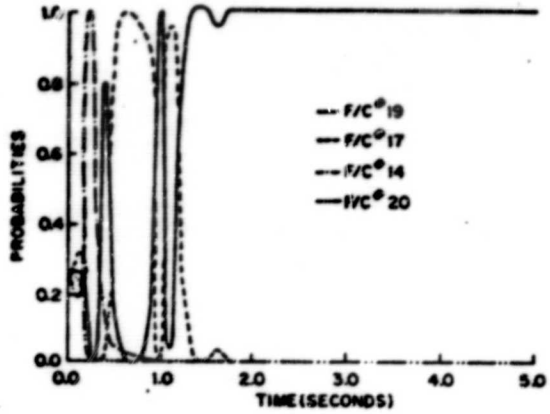

Figure 5 Probabilities Versus Time (true F/C #19 included) from Longitudinal Dynamics

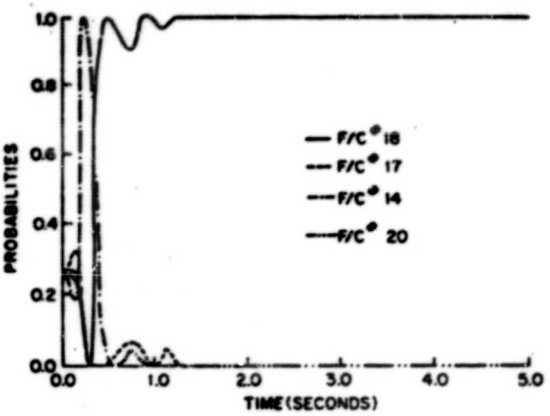

Figure 6 Probabilities Versus Time (true F/C #19 not included) from Longitudinal Dynamics

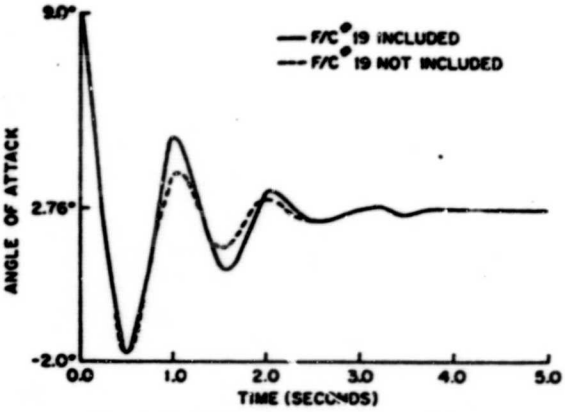

Figure 7 Angle of Attack Versus Time; Longitudinal Information Only

Appendix A

Wind Disturbance Model

As remarked in Sections 2 and 3, a continuous time wind disturbance model was included for both the lateral and longitudinal dynamics, corresponding to a state variable w(t). In this appendix we give the mathematical details of this model which was kindly provided by Mr. J. Elliott of NASA/LRC, as a reasonable approximation to the von Karman model and the Haines approximation. It is important to realize that the wind disturbance model changes from flight condition to flight condition. The power spectral density of the wind disturbance is given by

$$\text{(A.1)} \quad \Phi_g = \frac{\sigma^2}{\pi} \frac{L}{V_o} \left(\frac{4}{4 + \left(\frac{L}{V_o} \omega \right)^2} \right)$$

where L, the scale length, is

$$\text{(A.2)} \quad L = \begin{cases} 200 \text{ ft at sea level} \\ 2500 \text{ ft when altitude} > 2500 \text{ ft} \\ \text{linearly interpolated in between} \end{cases}$$

V_o is the speed of aircraft in ft/sec, ω in rad/sec, and

$$\text{(A.3)} \quad \sigma = \begin{cases} 6 \text{ ft/sec normal} \\ 15 \text{ ft/sec in cumulus clouds} \\ 30 \text{ ft/sec in thunderstorms} \end{cases}$$

To obtain a state variable model, a normalized state variable w(t) (in rad) is used as the wind state for both lateral and longitudinal dynamics. The state variable w(t) is the output of a first order system driven by continuous white noise $\xi(t)$ with zero mean. Thus the dynamics of the wind disturbance model are give by

$$\text{(A.4)} \quad \dot{w}(t) = -2\left(\frac{V_o}{L}\right) w(t) + \frac{2\sigma}{\sqrt{\pi L V_o}} \xi(t)$$

where $\xi(t)$ is zero mean white noise with unity covariance function

$$\text{(A.5)} \quad E\left\{\xi(t)\xi(\tau)\right\} = \delta(t-\tau)$$

The design was obtained for the intermediate case σ = 15 (cumulus clouds).

For the longitudinal dynamics the wind state w(t) influences the dynamics in the same manner as the angle of attack. Thus, in the longitudinal state equations the wind state w(t) enters the equations as follows

$$\text{(A.6)} \quad \begin{cases} \dot{q}(t) = \ldots\ldots\ldots + a_{13} w(t) \\ \dot{v}(t) = \ldots\ldots\ldots + a_{23} w(t) \\ \dot{\alpha}(t) = \ldots\ldots\ldots + a_{33} w(t) \end{cases}$$

where a_{13}, a_{23}, a_{33} can be found from the open loop longitudinal $\underline{A}$ matrix [2].

In the lateral dynamics the wind state w(t) influences the dynamics in the same manner as the sideslip angle. Thus, in the lateral state equations the wind state w(t) enters the equations as follows

$$\text{(A.7)} \quad \begin{cases} \dot{p}(t) = \ldots\ldots\ldots + a_{13} w(t) \\ \dot{r}(t) = \ldots\ldots\ldots + a_{23} w(t) \\ \dot{\beta}(t) = \ldots\ldots\ldots + a_{33} w(t) \end{cases}$$

where a_{13}, a_{23}, a_{33} can be found from the open loop lateral $\underline{A}$ matrix [2].